Proceedings of the 17th World Congress
The International Federation of Automatic Control
Seoul, Korea, July 6-11, 2008

Modelling, Parameter Identification and Dynamics Analysis of a Common Rail Injection System for Gasoline Engines

Matteo Corno*, Sergio M. Savaresi*, Riccardo Scattolini*
Emilio Comignaghi, Marco Sofia**, Antonio Palma***, Eduardo Sepe*****

**Dipartimento di Elettronica e Informazione, Politecnico di Milano, Piazza L. da Vinci, 32, 20133 Milano, ITALY (Tel: +39.02.2399.3545; e-mail: savaresi@ elet.polimi.it).*
*** FIAT Powertrain Technologies S.p.A., Viale Alfa Romeo, 20020 Arese (Milano), ITALY.*
**** Élasis S.C.p.A, Gasoline EMS Dpt., Via ex Aeroporto s.n., 80038 - Pomigliano d'Arco (Napoli), ITALY*

Abstract: The topic of this paper is the modelling, parameter estimation and analysis of a common rail direct injection system of a gasoline engine. After a brief description of the system, an analytical first-principles simulator is developed. Model parameters are identified and the simulator is validated using real data. It is shown how this approach can be useful to make a "virtual" (simulator-based) definition of the system by discussing trade-offs in the choice of several parameters of the injection system. In this work mechanics, fluid dynamics, and control algorithms are analyzed as a whole, in a genuine and modern "co-design" approach.

1. INTRODUCTION

In this work we present a study on a Direct Common Rail Injection System of a gasoline engine.

The key to obtain a clean and efficient combustion in ICEs (Internal Combustion Engines) lies in accurate control of the amount of combustible and air that are burnt in the chamber.

During the late 90's the Common Rail Injection System technology [Chiavola, Stumpp, Gauthier (2005)] was introduced for diesel engines. This technology's core is the common rail, a steel manifold where the fuel is kept at high pressure. Thanks to this technology it is possible to mix fuel and air directly in the combustion chamber and their mixture ratio can be controlled with much higher precision than in older technologies. In the last few years the common rail technology has been extended to gasoline engines [Alabastri, D'Errico, Li]. Gasoline direct injection engines owe their success to the increased fuel efficiency and performances that they can deliver.

These advantages come at the cost of a more complex system, both in the mechanics and in the electronics. Because of this higher complexity, it is increasingly more difficult to foretell the effects of a change in one of the parameters of the injection system. Hence the availability of a reconfigurable dynamic simulator can be a powerful aid in designing such complex systems. It can speed up the design process while cutting down the development costs by strongly reducing the trial-and-error procedure on engine prototypes.

The goal and scope of this work is to show a modern and important industrial example where mechanics, fluid-dynamics, gray-box system identification and automatic control are considered as a whole, in a genuine "system" co-design approach and to show how a virtual prototype can be used to study different system configurations.

The work is structured as follows. Section 2 describes the overall architecture of the system. The mathematical model of the system is derived from basic fluid dynamics principles in Section 3. In Section 4, the simulator is used to study the role of several system parameters.

The work presented herein is entirely based on an early prototype of a gasoline direct ignition turbocharged engine of Fiat Powertrain Technologies, developed for the Alfa Romeo brand.

2. COMMON RAIL INJECTION SYSTEM

The Common Rail Injection System is a hydraulic circuit that connects the fuel tank to the piston chambers of the engine. Its goal is to deliver the requested amount of fuel to the injectors, at the desired (high) pressure.

The system is schematically depicted in Fig. 1. Roughly speaking, the system is divided into two main sections: the low-pressure and the high-pressure circuits. The analysis of the low-pressure circuit is out of the scope of this work. The most interesting part is the high-pressure circuit; it starts with the high-pressure pump, and ends at the injectors. Its main elements are now briefly described:

HIGH PRESSURE PUMP. It is a volumetric pump that connects the low-pressure circuit to the high-pressure one. It compresses the gasoline from 6 bar to [30-150] bar, according to the working load and speed. The piston of the pump is mechanically connected to the camshaft through a cam-following system.

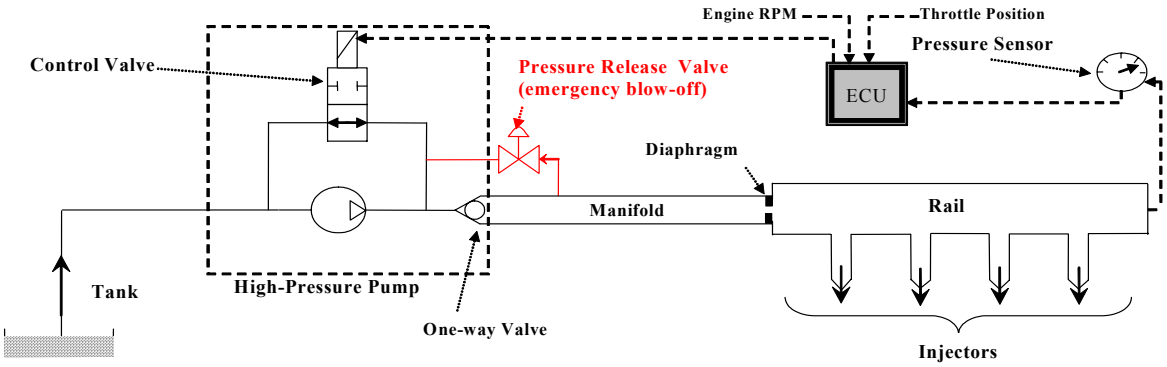

Fig. 1.The Common Rail Injection system architecture.

In modern common rail systems, the pressure control is achieved through a control valve built in the high-pressure pump. The pump is constituted of three main functional elements: the piston, the control valve and the one-way valve. The control valve allows to redirect the output of the pump toward the low-pressure circuit. It has only two possible states: open or closed.

The pump operates by periodically alternating an aspiration and a compression phase. During aspiration the piston moves downward and the control valve is open. The gasoline flows from the low pressure circuit into the pump chamber. In the compression phase the piston moves upward; initially the control valve is open. The gasoline hence flows back to the low pressure circuit. At any time in this phase the controller can command the closing of the valve. When the valve closes, the pressure in the chamber increases; once it is equal to the pressure in the manifold the one-way valve opens and the gasoline is pumped in the high-pressure manifold. According to this control logic the control variable is the closing instant of the control valve.

MANIFOLD. It is a pipeline connecting the outlet flange of the high-pressure pump to the common rail.

*DIAPHRAGM***.** The common rail and the manifold are connected through a diaphragm. The role of this component is to obtain better damping of the system and a partial decoupling between the pressures of the manifold and the pressure of the rail.

COMMON RAIL. It is the core of the system. It is connected to the manifold through the diaphragm. Since the injectors are connected to the common rail, the main control objective is to regulate the rail pressure at the desired reference value, without oscillations.

3. SYSTEM MODELING

In this section the mathematical model of the high-pressure injection system is briefly described. The model belongs to the class of 1-Dimensional models (1 spatial variable is explicitly considered); henceforth, it is described by partial derivative differential equations. It has been recast into a lumped-parameter system using a finite difference scheme. The developed model represents a good compromise between complexity and accuracy.

The injection system is obtained by connecting several hydraulic elements; moreover, in order to obtain a complete dynamic simulator of the system, the closed-loop pressure control algorithm must be modelled too. The model equations used for these subsystems are now briefly outlined.

PIPELINES (MANIFOLD, RAIL). The most important dynamic phenomenon of the system is the propagation of pressure waves in a fluid contained in elastic, circular constant section pipelines. The pipeline model is given by gasoline mass and momentum balance along the principal dimension of the pipe ([Alabastri, Thomas]).

$$\begin{cases} \dfrac{A}{c^2}\dfrac{\partial P}{\partial t}+\dfrac{\partial w}{\partial x}=0 \\ \dfrac{\partial}{\partial t}\left(\dfrac{w}{A}\right)+\dfrac{\partial}{\partial x}\left(\dfrac{w^2}{A^2\rho}\right)+\dfrac{\partial P}{\partial x}+F_f=0 \end{cases} \tag{1}$$

In (1) ρ is the gasoline density expressed in kg/m^3; w is the gasoline mass flow expressed in kg/s; P is the gasoline pressure expressed in Pa; c is the sound velocity in the fluid expressed in m/s; A is the section area of the pipe expressed in m^2; F_f is the load loss due to friction. The sound velocity term c depends on the properties of the fluid and the elasticity of the pipe. It is given by:

$$c=\sqrt{\frac{\beta}{1+K\beta}\frac{1}{\rho}} \tag{2}$$

where β is the bulk modulus that describes the compressibility of the fluid and K is the stiffness of the pipe that depends on its material and on its geometric properties. In addition, assuming turbulent flow (this assumption will be verified a-posteriori) the frictional load loss can be written as:

$$F_f=2\frac{w|w|}{\rho A^2 D^2}f\ , \tag{3}$$

where D is the inner diameter of the pipe and f is the pipe Fanning friction factor. Heat exchange phenomena are neglected in the model. While thermal interaction within different parts of the systems happens, its dynamics are much slower than wave propagation. The final model is a system of two partial differential equations. This infinite-dimensional system is transformed in a finite-dimensional one by means of the finite-difference method ([Bertin, Strikwerda]). The

pipeline is divided in N cells each assumed to have a uniform pressure and an inflow and outflow.

The finite-difference approximations used herein are:

$$\frac{\partial P}{\partial x} \approx \frac{P(i+1)-P(i)}{\Delta x} \qquad \text{for } i = 1 \ldots N \qquad (4)$$
$$\frac{\partial w}{\partial x} \approx \frac{w(i)-w(i-1)}{\Delta x}$$

In (4) Δx represents the cell length; $P(i)$ is the mean pressure within the i-th cell; $w(i)$ and $w(i-1)$ are the inlet and the outlet flows of the i-th cell, respectively, and N is the number of cells.

The set of equations (4) must be complemented with boundary conditions. For the rail, complete reflection of the wave at the end of the rail is assumed while the inlet flow is equalled to the outlet flow of the diaphragm. Different boundary conditions are needed for the manifold because it is open on two sides. Its boundary conditions are expressed in term of inlet flow (equalled to the outlet flow of the high pressure pump) and the outlet flow which is equal to the inlet flow of the diaphragm.

DIAPHRAGM. The diaphragm is a narrowing of the pipe. It is mainly used to increase the overall damping of the system, and to decouple the manifold and the rail dynamics. The narrowing is coaxial to the fluid flow; thus it acts as a concentrated load loss. Since the length of the diaphragm is comparable to the length of a single cell, it has been decided to model the diaphragm as a constant aperture valve with an internal capacity (similarly to a single cell of the rail or manifold) [Thomas]. It is important to notice that the model must be able to manage inversion of the flow. This calls for a variable step integration routine; the choice fell on ODE 15 that can treat stiff systems.

INJECTORS. The injectors are modelled as outlet valves, connected to the rail. According to their control technology, the opening request of the injector is assumed to be a two-valued variable (open-closed). The dynamics of the orifice area are approximated by a first order filter with a pure delay. The relationship between the actual orifice area and the output fuel flow is assumed to be a non-dynamic relationship. The map between rail pressure and the output injector flow is modelled by a static quadratic function.

HIGH PRESSURE PUMP AND THE CONTROL VALVE. The high-pressure pump is modelled as a flow source connected to the first cell of the manifold. The compression dynamics inside the pump chamber can be neglected because the volume of the chamber is negligible with respect to the volume of the rest of the system. Being the piston connected to the engine camshaft via a cam-follower system, the instantaneous gasoline flow is determined by the profile of the cam. Specifically:

$$w_{Pout} = 0 \quad \text{if control = open}$$

$$w_{Pout} = \rho A_{pist} \frac{dh}{dt} \quad \text{if control = closed.}$$

Where A_{pist} is the area of the piston; h is the height of the piston and control is the state of the control valve.

Three different cam profiles are taken into account; they are shown in Fig. 2. The number of lobes of the profile is an important characteristic because it determines the number of blows that the pump delivers for each revolution of the camshaft.

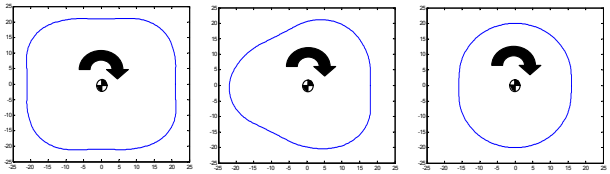

Fig. 2. High pressure pump cam profiles (4-lobes, 3-lobes, 2-lobes).

CONTROL ALGORITHM. Although several advanced control schemes are available in the literature [Gauthier (2007)], in this industrial application rail pressure regulation is achieved via a classical proportional integral (PI) controller scheduled on the RPM and a feed-forward component which is used to compensate for the estimated injected gasoline. The control variable is the closing time of the valve. It determines the gasoline flow toward the rail. Hence, this actuator implements a sort of Pulse-Width-Modulation (PWM). The duty-cycle of this PWM is an entire cam-shaft cycle; however, only half of this cycle is available for control. The aspiration phase is a pure delay. Also in this case, notice that the duty-cycle is time-varying but camshaft-angle-invariant.

The injection system model contains many parameters. They can be clustered into two classes: geometric and fluid-dynamics parameters. Geometric parameters are easily and precisely measured; fluid dynamics parameters could not be directly measured and were experimentally estimated. The estimated parameters, namely the bulk modulus and the Fanning friction coefficient, take into account all the uncertainties and model simplifications as a whole; this approach in the System Identification literature is knows as "gray-box" approach (see e.g. [Dunstan] and references cited therein). The identification results can be appreciated in Fig. 3, where the measured and simulated pressures (manifold and rail) are displayed at 4000 RPM and at full throttle. All pressures are normalized with respect to the control set point P_0.

By inspecting the simulation results, it is clear that the main resonances and the damping of the system are accurately modelled. The relevant dynamics are correctly captured. As a matter of fact notice that small oscillations at very high frequencies are reproduced by the model, but the fitting between the simulated and the measured data is poor. In order to improve the model accuracy beyond 1KHz a more complex model and experimental setup is needed. High accuracy in the high-frequency range however is out of the scope of this work, since it is not necessary for the analysis

described in the next section.
Note that the turbulent-flow assumption made on the model can be a-posteriori checked. By computing the highest flow speed under normal operation it is found that the maximum Reynolds number is about 45000; it is well above the limit (2000) that separates the laminar and turbulent flows.

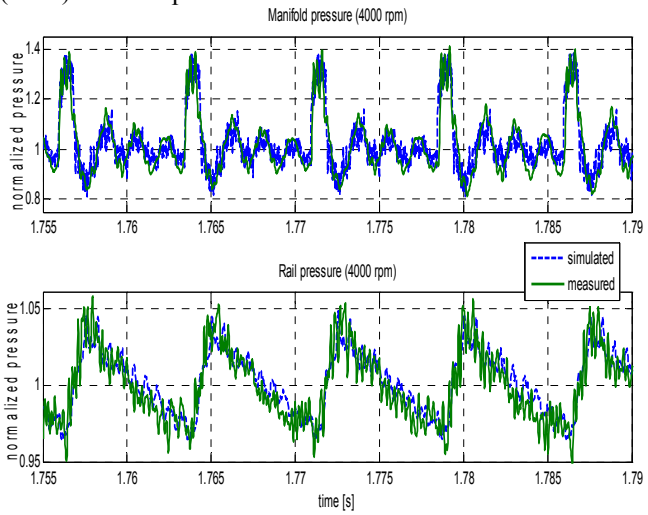

Fig. 3. Manifold and rail pressure at 4000 RPM.

4. SYSTEM CONFIGURATION ANALYSES

The availability of an easily reconfigurable model allows low-cost sensitivity analyses. This approach is usually called "virtual-prototyping". The simulator can be used in many different ways and with different purposes. In this work we focus on the design of the rail diameter, the manifold diameter and the cam of the high-pressure pump.

During the first test-bench runs of the prototype engine, it was observed that the pressure in the manifold reached values well above the safety release valve threshold set to 1.3 times the maximum nominal pressure. The virtual prototype allowed to find out that this problem is related to the diameter of the manifold. The results of the analysis of the effect of the manifold diameter on the peak-pressure in the manifold are condensed in Fig.4. The following remarks are due:

• Using the baseline manifold diameter, the blow-off valve is activated for engine speed above 3000 RPM.

• The pressure-peak problem worsen when the engine speed increases.

• The maximum pressure exhibits hyperbolic-like dependence on the diameter of the manifold.

Another important feature of the system is the rail diameter. The size of the rail plays a key role in determining the pressure variations around the nominal set-point. The analyses of the effect of rail diameter variations is condensed in Fig.5, where the peak-pressure in the manifold and the pressure variance in the rail are displayed as a function of the rail size, for two engine speeds. Notice that in the rail the pressure variance (around its nominal value) is the key performance index, whereas in the manifold the peak pressure is the right performance indicator. As a matter of fact the manifold problem is the activation of the blow-off valve; instead, in the rail, the objective is to keep the pressure variations as small as possible, since they decrease the precision of the amount of the injected fuel.

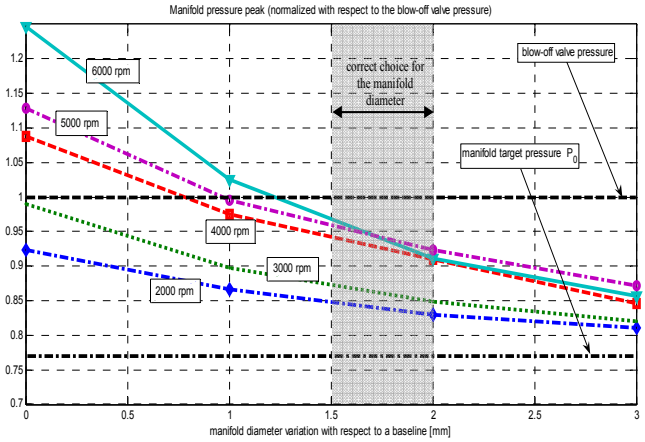

Fig. 4 Manifold maximum pressure as a function of the manifold diameter increment for different engine speeds.

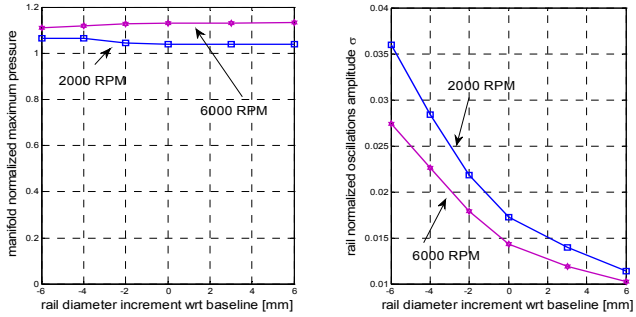

Fig. 5. Manifold normalized maximum pressure (left) and pressure oscillations in the rail (right) for different engine speeds and rail diameters.

From Fig.5 the following remarks are due:

• The manifold pressure peaks are weakly dependent on the diameter rail. This confirms that the diaphragm located between the manifold and the rail guarantees decoupling of the two ducts.

• The pressure oscillations in the rail are strongly related to the rail diameter. They monotonically decreases with increasing rail diameters.

• The pressure oscillations in the rail weakly depend on the engine speed. Notice, however, that the oscillation variance slightly decreases as the engine speed increases; this is due to the averaging effect of the longer injection time.

• The nominal (baseline) diameter rail used in the prototype engine is located on a "knee" of the curve; this means that further increasing the diameter provides a small reduction of oscillations, while reducing the diameter strongly increases

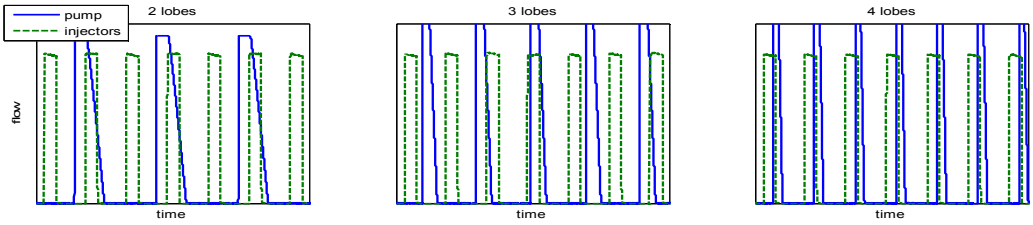

Fig. 6. Pumped and injected fuel flows for different cam profiles (2000 RPM)

the oscillations. It is important to remark that increasing the diameter has the clear advantage of reducing pressure variance, but it has also a drawback: the transient time required when the pressure set-point is changed. An analysis of the sensitivity of transient time to rail diameter shows that a 2 mm diameter variation can change the transient time of more than 20%. This analysis confirms the correct choice of the "baseline" rail diameter used in the prototype engine: increasing the diameter would cause a marginal reduction of the oscillations amplitude, but a significant increase of the rise time during transients; similarly, decreasing the diameter would significantly deteriorate the pressure variance, while marginally decreasing the rise time.

Another key element of the injection system is the high-pressure pump; it maintains the high pressure inside the common rail. Three different solutions are taken into account: 2, 3 and 4 lobes (see Fig. 2). The three configurations are characterized by the same cylinder area and the same pumped volume in a single engine-revolution.

Roughly speaking, a configuration with more lobes should provide a more uniform pressure profile; the drawback can be a high-frequency excitation, which may conflicts with the system resonances.

The synchronization of the pump blows and the injectors openings is a key issue to understand the effect of the pump and the injectors on the rail pressure. In Fig. 6 the input-output fuel flows for the three different cam profiles are illustrated, at 2000 RPM. Notice that:

• The 2-lobe and the 4-lobe configurations are characterized by a fixed phase relationship with respect to the injectors.

• The 3-lobes configuration is characterized by a time-varying phase relationship between the injection pulse and the pump pulse; due to the 3:4 ratio.

Since the phase relationship between the injector and the pump has a strong influence on pressure oscillations, in Fig. 7 the two extreme conditions are displayed in the time domain: the phase relationship which minimizes rail pressure oscillation (labelled as "best phase"), and the phase relationship which maximizes rail pressure oscillation (labelled as "worst phase").

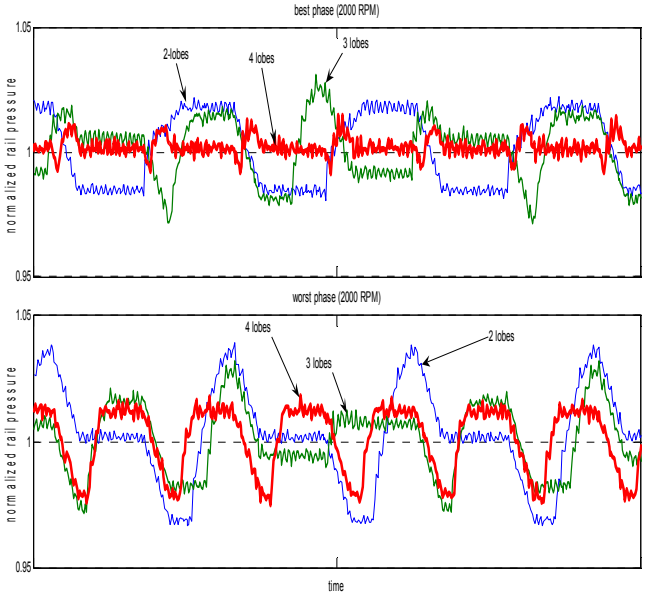

Fig. 7. Normalized rail pressure for different cam profiles and for different pump-injector phases.

The following remarks are due:

• In the 4-lobes and in the 2-lobes configurations, the difference between the best phase and the worst phase is remarkable.

• The pressure variance of the 3-lobes configuration is almost insensitive to the phase shift; this is due to the fact that, thanks to the 3:4 ratio, the relative phase shift is time-varying; this results in an "averaging" effect.

The worst/best case analysis presented in detail in Fig. 7 for the 2000 RPM speed has been extended to the whole speed range; the results are condensed in Fig. 8. The following comments can be done:

• The "best phase" condition can be easily interpreted: the higher the number of lobes is, the lower the oscillations are; this holds for any engine speed.

• The "worst phase" condition is less obvious: the 2-lobe configuration is the worst, for any engine speed. The 4-lobe and the 3-lobe configuration provide very similar performance.

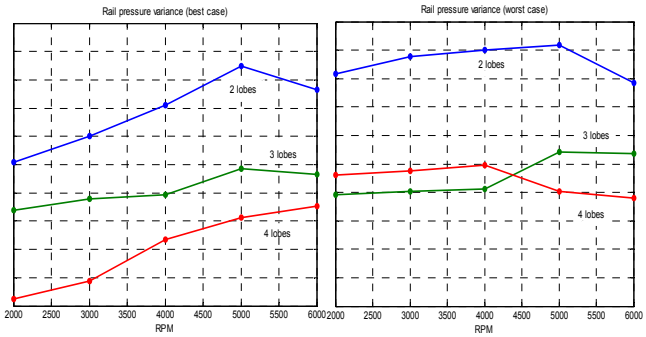

Fig. 8. Rail pressure variance, for different configurations. Left: best phase. Right: worst phase.

The pressure variance around the nominal value is the main performance index. Another aspect, however, must be considered: the phase lag introduced by the pump in the pressure regulation control loop. This issue is less evident and more subtle, but it can be critical, especially at low engine speed.

As explained in detail in Section 2, the fuel flow pumped in the high-pressure manifold is modulated by selecting the time instant when the control valve is closed. The control action can be applied only within the compression phase, whereas the aspiration phase is a "dead-zone" for the actuator. The effect of this peculiar feature is that the aspiration phase acts as a time-varying (but angle-invariant) pure delay in the control loop. Apparently, such a delay depends on the number of lobes of the pump. In camshaft angle this pure delay corresponds to 45°, 60°, and 90°, for the 4, 3, and 2-lobe configurations, respectively.

In the frequency domain the pure delay translates into a phase-margin loss in the loop-function. At comparatively low engine speed (in the 1000-2000 RPM range) the phase loss due to the aspiration "dead-zone" is not negligible, reaching 35° at 1000 RPM for the 2-lobes configuration.

Since the pressure-regulation control loop is critical from the phase-margin point of view, this analysis clearly indicates the need of a speed-scheduled controller. At low engine speed the controller bandwidth must be decreased, in order to compensate the phase loss due to the effect of the pure-delay of the aspiration dead-zone; at high engine speed a larger closed-loop bandwidth can be achieved.

The results of this analysis of three different pump configurations can be summarized as follows:

• The 2-lobe configuration is critical both in terms of phase-margin loss and pressure oscillations.

• The 4-lobe configuration provides the best results both in terms of phase-margin loss and pressure oscillations; however, in order to achieve the best possible performance the phase relationship between the pump and the injectors should be accurately tuned as a function of the engine speed.

• The 3-lobe configuration can provide an interesting compromise: the phase-margin loss is acceptable, and, on an average-case basis, it guarantees the same pressure-variation performance of the 4-lobe configuration.

5. CONCLUSIONS

The focus of this work has been on providing an easily reconfigurable simulation tool that can help speed up the design process of the injection system for a gasoline engine.

In the second part of the work, it has been shown how the simulator can be used to assess the effect of several important design parameters. The analyses allowed to draw useful guidelines for the design of such a complex system.

REFERENCES

Alabastri E., L. Magni, S. Ozioso, R. Scattolini, Other (2004). Modeling, analysis and simulation of a gasoline direct injection system. In: *"Proceeding of First IFAC Symposium on Advances in Automotive Control"* Salerno, 2004.

Baker P., H. Watson, (2005). MPI air/fuel mixing gaseous and Liquid PLG. In: *"SAE Technical Papers"*, 2005-01-0246.

Bertin, D., S. Bittanti, S.M. Savaresi (2000). The decoupled cushion control in ride control systems for air cushion catamarans. In: *"Control Engineering Practice"*, vol.**8**, pp 191-203.

Chiavola O., Giulianelli P (1999). Modeling and simulation of common rail systems. In: *"SAE Technical Paper 1999-01-0199"*.

D'Errico G., Onorati A. (2004). An integrated simulation model for the prediction of GDI engine cylinder emissions and exhaust after-treatment system performance. In: *"Proceeding of SAE Int. Congress & Exp"* Detroit, Michigan, USA.

Gauthier C., Sename O., Dugard L., Meissonier G. (2005). Modelling of a diesel engine common rail injection system. In: *IFAC 16th World Congress,* Prague.

Gauthier C., Sename O., Dugard, L., Meissonier G. (2007). An Hinf linear parameter varying controller for a diesel engine common rail injection system. In: E*uropean Control Conference*, Kos, Greece.

Li J. Z., Treusch C., Honel B., Neyrat S. (2005). Simulation of pressure pulsations in a gasoline injection system and development of an effective camping technology. In *"SAE Techical Paper, 2005-01-1149"*

Dunstan W., R.R. Bitmead, S.M. Savaresi (2001). Fitting nonlinear low-order models for combustion instability In *"Control Engineering Practice"*, vol. **9**, pp.1301-1317.

Strikwerda J. (1989). *Finite difference schemes and PDE*. Wadsworth Brooks/Cole.

Stumpp G., Ricco M J. (1996). Common Rail – An attractive fuel injection system for passenger car DI diesel engine. In: "*SAE Technical Paper*", 1996-08-0070.

Thomas P. (1999). *Simulation of industrial processes for control engineers*. Butterworh Heinemann, Oxford, England.